ISSN 1063-7842, Technical Physics, 2015, Vol. 60, No. 5, pp. 724–729. © Pleiades Publishing, Ltd., 2015.
Original Russian Text © D.M. Sedrakyan, P.G. Petrosyan, L.N. Grigoryan, 2015, published in Zhurnal Tekhnicheskoi Fiziki, 2015, Vol. 85, No. 5, pp. 94–99.

PHYSICS
OF NANOSTRUCTURES

Effect of Random Potential on the Optical Properties of the CdS_xSe_{1-x} Semiconductor Nanocrystals

D. M. Sedrakyan, P. G. Petrosyan*, and L. N. Grigoryan

Yerevan State University, ul. Aleka Manukyana 1, Yerevan, 0025 Armenia
**e-mail: ppetros@ysu.am*

Received March 13, 2014

Abstract—CdS_xSe_{1-x} semiconductor crystals in silicate glass with different degrees of perfection of crystalline lattice are fabricated. The spectral features of the optical transmittance and photoluminescence at the initial stage of the heat treatment cannot be interpreted using only the diffusion growth of nanocrystals. Structural defects of nanocrystals must be taken into account at the initial stage of the crystal growth.

DOI: 10.1134/S1063784215050230

INTRODUCTION

A new branch of the semiconductor physics is related to the study of the optical and electric properties of the smallest semiconductor crystals with sizes of several nanometers [1–3]. Recent interest in the semiconductor nanocrystals in silicate glass has been driven by the applications in optoelectronic devices [4–6].

In comparison with bulk semiconductors, nanocrystals exhibit limitations on the motion of electrons and, hence, energy quantization. The positions of discrete energy levels depend on the size and shape of nanocrystals [7, 8]. The calculations of the energy spectra are normally performed with allowance for the distribution of the periodic energy potential and the limitations on the motion of electrons in the presence of a periodic field. However the electron microscopy [9–11] shows imperfect crystal lattice at the initial stage of the nucleation in nanocrystals. Thus, nanocrystals exhibit both periodic and random potentials that contribute to the formation of the band structure. In our opinion, the effect of the random potential on the band structure and, hence, the optical properties of semiconductor nanocrystals is of practical and scientific interest.

In this work, we study the effect of random potential on the optical properties of the CdS_xSe_{1-x} semiconductor nanocrystals in silicate glass.

RESULTS AND DISCUSSION

The CdS_xSe_{1-x} nanocrystals in silicate glass were fabricated using the procedure of [12]. The samples differ from each other by mean sizes of nanocrystals. Semiconductor nanocrystals with different sizes and degrees of perfection of crystal lattice are grown at a fixed temperature and time of heat treatment of silicate glass. The heat treatment is performed in a computer-controlled oven at a temperature of 530°C. The temperature of the heat treatment is reached over one hour, and, then, the samples are stored at a constant temperature. The annealing of glasses leads to staining, so that the glass colors range from light yellow to dark red.

The transmission and photoluminescence spectra are studied in the wavelength interval 300–900 nm using Ocean optics USB-4000 and Cary Eclipse fluorescence spectrometers.

Figure 1 shows the transmission spectra of the samples that are measured prior to and after heat treatment in air (sample T_1 is not thermally processed and the processing times of samples T_2–T_8 at a temperature of 530°C are $t_2 = 5$ min, $t_3 = 15$ min, $t_4 = 35$ min, $t_5 = 65$ min, $t_6 = 125$ min, $t_7 = 245$ min, and $t_8 = 425$ min). It is seen that the heat treatment leads to the formation of a sharp absorption edge and the red shift of the absorption edge. Additional heat treatment also causes variations in the transmittance of the samples: an increase at the initial stage is followed by a decrease. A variation in the spectral shape and the edge shift are due to the formation of nanocrystals and the further diffusion growth [13]. Using the transmission spectra, we can determine the mean size of semiconductor nanocrystals. The experimental transmission spectra make it possible to calculate the spectral dependence of absorption coefficient $K = K(h\nu)$. The experiments yield minor (less than 4%) reflectance for a wavelength interval of 350–700 nm. Thus, the reflection can be disregarded in the analysis of quantity $K = K(h\nu)$.

The CdS_xSe_{1-x} semiconductor exhibits the direct-band-gap structure, so that the spectral dependence of the absorption coefficient is given by

$$K = \frac{A}{h\nu}(h\nu - E_g)^{1/2}, \quad (1)$$

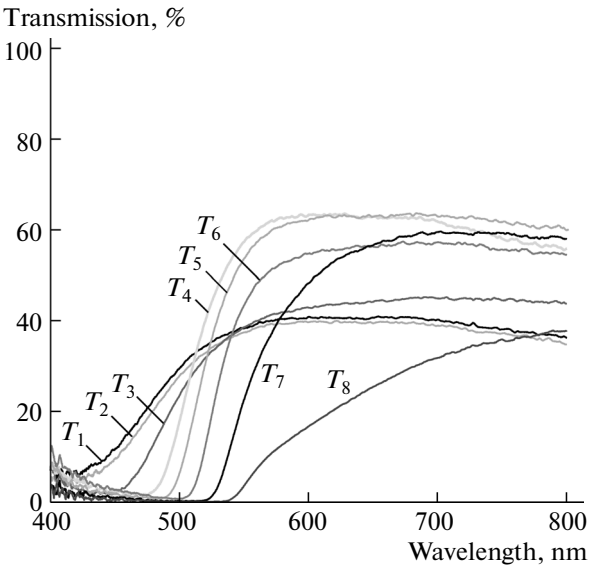

Fig. 1. Transmission spectra of silicate glasses containing CdS_xSe_{1-x} semiconductor nanocrystals (sample T_1 is not thermally processed and the processing times of samples T_2–T_8 at a temperature of 530°C are $t_2 = 5$ min, $t_3 = 15$ min, $t_4 = 35$ min, $t_5 = 65$ min, $t_6 = 125$ min, $t_7 = 245$ min, and $t_8 = 425$ min).

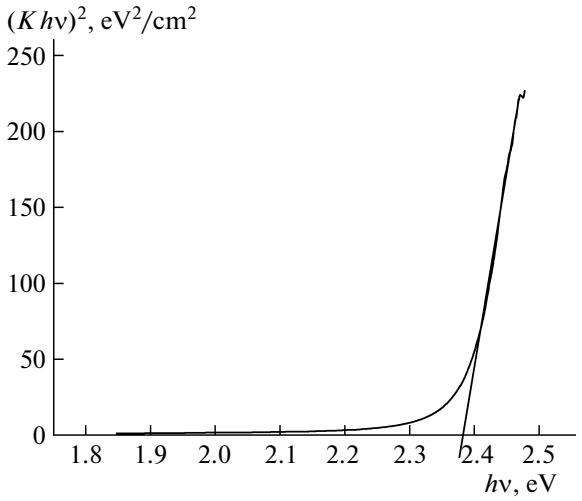

Fig. 2. Plot of quantity $K = f(h\nu)^2$ vs. energy of incident photon for sample T_6.

where parameter A = const depends on the effective masses of electrons and holes, $h\nu$ is the energy of the incident photon, and E_g is the band gap. Figure 2 presents an example of the dependence $K = f(h\nu)^2$. The analysis of the absorption spectra shows that the spectra exhibit exponential fragments at $h\nu < E_g$ and the square-root dependence at $h\nu > E_g$. Using the point of intersection of the linear fragment of the dependence $K = f(h\nu)^2$ and the abscissa axis, we can determine energy $h\nu_{0.1}$ that corresponds to the transitions between the first energy levels for electrons and holes that result from the quantum dimensional effect. For spherical quantum dots the sizes of which are no greater than the exciton radius, parameter $h\nu_{0.1}$ is represented as [15]

$$h\nu_{0.1} = E_{g0} + \frac{\hbar^2\pi^2}{2\mu R^2}, \qquad (2)$$

where E_{g0} is the band gap for the bulk sample, $\mu = \frac{m_n m_p}{m_n + m_p}$, and R is the mean radius of the quantum dot.

The mean radii of nanocrystals in the samples that were processed at different processing times are determined with the aid of expression (2). To determine the mean radius of nanocrystals, we need energy E_{g0}, which depends on parameter x of the CdS_xSe_{1-x} compound. It is well known that the phase decay contains three stages: nucleation, diffusion growth, and coalescence (final stage). At the final stage, the sizes of relatively large crystals increase due to the absorption of small crystals [16, 17]. An increase in the time of heat treatment may lead to the formation of crystals with sizes that make it possible to neglect the effect of size quantization. In such samples, the band gap tends to E_{g0}. The experiments show that the band gap tends to a level of 2 eV due to the long-term heat treatment.

The width of the interval of the square-root dependence of the absorption coefficient is determined by the parabolic dependence of the carrier energy on wave vector $E(k)$. When the sizes of nanocrystals increase, the energy spectrum becomes closer to the spectrum of the bulk CdS_xSe_{1-x} sample. For increasing sizes of nanocrystals, the width of the interval of the square-root dependence must increase. Such a width m is given by $m = h\nu_0 - h\nu_\Delta$, where $h\nu_\Delta$ is the energy at which the square-root dependence is started and $h\nu_0$ is the maximum photon energy at which the dependence vanishes. Figure 3 shows the width of the interval of the square-root dependence versus the size of nanocrystals. It is seen that the expected increase is observed up to a certain size of nanocrystals and, then, the width decreases. Note that such a decrease takes place when the transparency of the samples decreases.

A deviation from the square-root dependence $K = f(h\nu)$ is observed at low frequencies. When the annealing time increases, interval Δ ($\Delta = h\nu_\Delta - E_g$, where $h\nu_\Delta$ is the photon energy at which dependence $K = f(h\nu)^2 = f(h\nu)$ reaches the linear fragment), which characterizes the deviation, decreases (Fig. 4). For semiconductor, the exponential dependence of the absorption coefficient at energies $h\nu < E_g$ results from violations of periodicity of the crystal-lattice potential. For the system under study, parameter Δ, which characterizes the broadening of the absorption edge, can be determined by the variance of the nanocrystal radius and the presence of point defects [18]. A decrease in quantity Δ at the initial stage of the heat treatment indicates that the

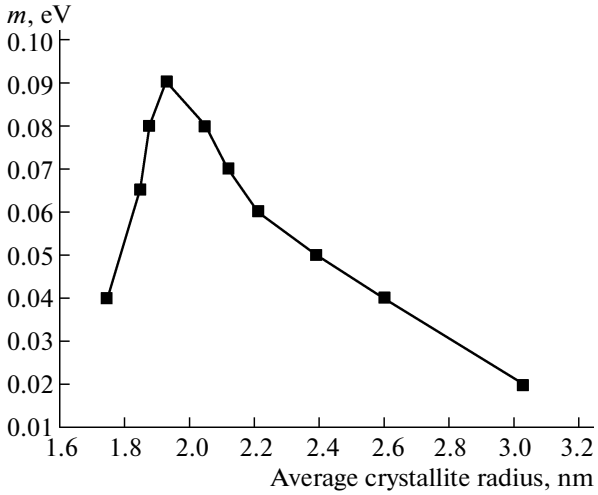

Fig. 3. Plot of the width of the interval of square-root dependence vs. size of nanocrystals.

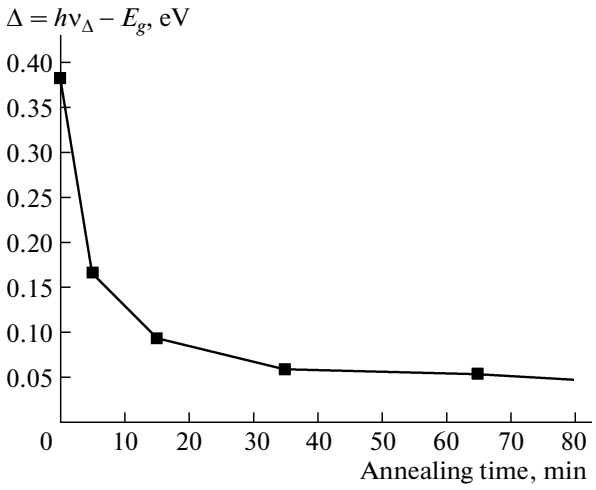

Fig. 4. Plot of parameter Δ vs. annealing time.

annealing leads to a decrease in the degree of perfection of the crystal lattice.

The structural changes in nanocrystals must also be manifested in the photoluminescence spectra. We study the photoluminescence spectra of the samples that differ from each other by the durations of additional heat treatment at a temperature of 530°C. A mercury lamp with a radiation wavelength of 250 nm serves as the excitation source in the measurements of the photoluminescence spectra in a wavelength interval of 300–900 nm.

Figure 5 shows the photoluminescence spectra of silicate glasses with the CdS_xSe_{1-x} nanocrystals at several excitation powers. The radiation power is controlled using the supply voltage of the mercury lamp. It is seen that the photoluminescence is relatively weak at the initial stage of the annealing, which can be due to the absence of the perfect crystal lattice at the initial stage and, hence, the nonradiative recombination. When the annealing time increases, the photoluminescence intensity, first, increases and, then, decreases. Figure 6 presents the dependence of the maximum photoluminescence intensity on the mean size of nanocrystals at a supply voltage of the mercury lamp of 750 V. The edges of the absorption and photoluminescence spectra, which correspond to the recombination of carriers to lower energy levels or smaller traps, are red-shifted with an increase in the annealing time. The photoluminescence at wavelengths that are greater than the wavelength corresponding to the edge of the absorption band is related to the recombination of carriers on traps [19]. The traps are localized at the semiconductor–glass interface or semiconductor surface. The surface traps can be related to the Cd^{2+}, S^{2-}, and Se^{2-} vacancies or adsorbed oxygen ions on the semiconductor surface. A decrease in the transparency, the width of the square-root dependence, and the maximum luminescence intensity for the samples with relatively large nanocrystals are presumably due to the formation of new defects on the semiconductor–matrix interface and semiconductor surface owing to multiple heat treatment of a single sample. We plan additional study to substantiate the assumption.

Figure 7 shows the dependence of the mean size of nanocrystals on the time of heat treatment at a temperature of 530°C. The mean size of nanocrystals is determined in the approximation that the electron and hole bands are parabolic, and the electron–hole interaction (formula (2)) is disregarded. It is known that the nucleation is followed by the diffusion growth of nanocrystals. In the course of the diffusion growth, the dependence of the mean radius on the time of heat treatment is given by [11, 17]

$$R(t) = R_0 + \sqrt{2D\frac{C_0 - C_e}{C_p - C_e}t}, \qquad (3)$$

where C_0 is the concentration of the semiconductor phase in the matrix at the beginning of the process, C_e is the equilibrium concentration of the semiconductor phase in the matrix, C_p is the semiconductor concentration in nanocrystal, and D is the effective diffusion coefficient. The experimental dependence of the mean size of nanocrystals on the time of heat treatment was approximated using the formula $R(t) = R_0 + k\sqrt{t}$ and the following results were obtained: $R_0 = 18.3$ Å and $k_0 = 0.5$ Å/min$^{1/2}$. Figure 6 shows that the square-root dependence is observed at $t > 50$ min. A sharp increase in the size of nanocrystals at the initial stage of heat treatment cannot be interpreted using the diffusion process.

The energy of the ground state of a cylindrical quantum particle that is dispersed in a transparent dielectric matrix was analyzed in [20]. For a nanostructure that contains a point defect (δ-function

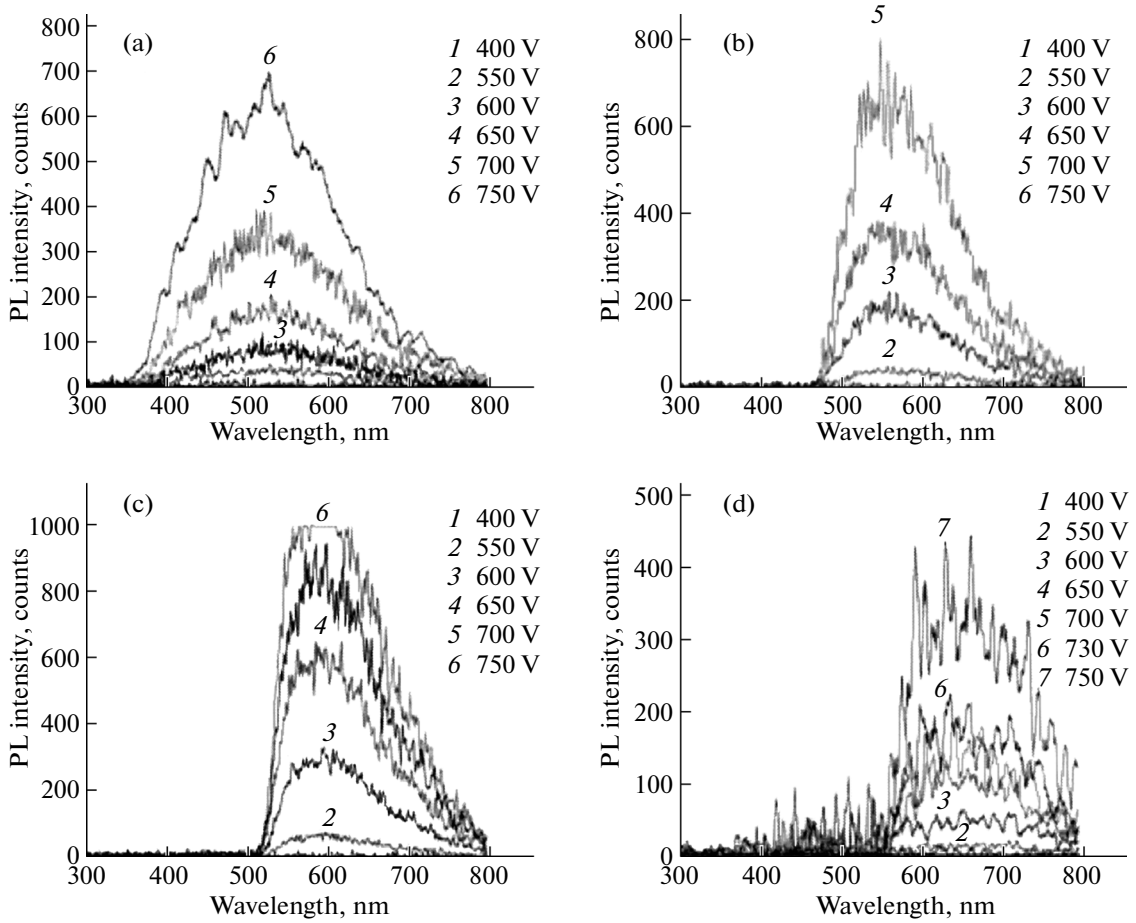

Fig. 5. Photoluminescence spectra of silicate glasses with the CdS_xSe_{1-x} nanocrystals: (a) prior to heat treatment, and after heat treatment at a temperature of 530°C at annealing times of (b) 5, (c) 35, and (d) 125 min.

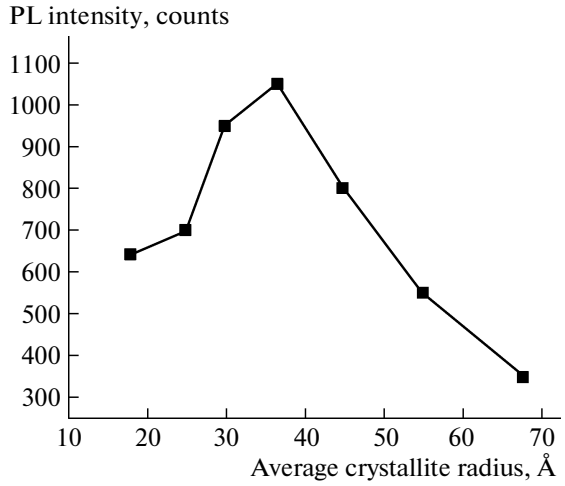

Fig. 6. Plot of the maximum photoluminescence intensity on the mean size of nanocrystals.

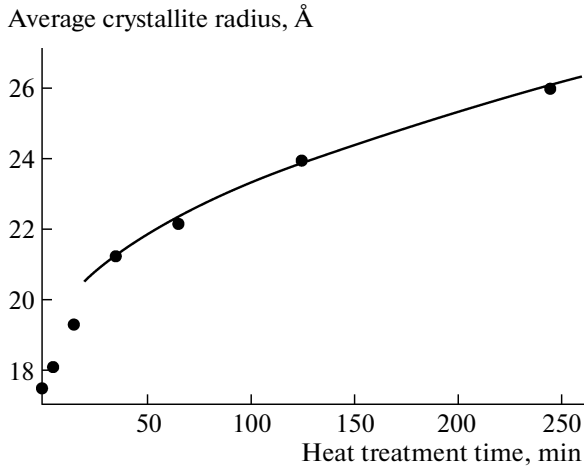

Fig. 7. Plot of the mean size of nanocrystals vs. time for a temperature of 530°C.

potential), the dependence of the edge of the absorption band on the position and amplitude of the δ-shaped potential was determined. The nanocrystal in the dielectric matrix represents a 3D infinite potential well for carriers. Spherical nanocrystals are predominantly employed in the study of the energy spectrum of carriers in nanocrystals. In this case, the analysis of the energy levels is reduced to the solution of a conven-

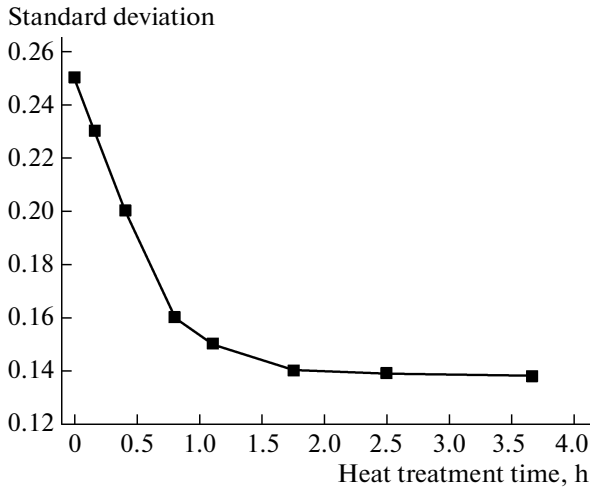

Fig. 8. Plot of the variance of nanocrystals vs. heat-treatment time.

tional problem that involves the stationary motion of a particle in a spherically symmetric rectangular well with an infinite depth. The absorption edge (for $R \ll a_B$, where a_B is the Bohr radius), which is determined by the transitions between the main quantum levels of electrons and holes, is calculated using formula (2).

The results of electron microscopy [21] show that the CdS_xSe_{1-x} nanocrystals in silicate glass exhibit an elongated rather than spherical shape. The X-ray diffraction shows that the CdS_xSe_{1-x} particles in silicate glass exhibit hexagonal structure with lattice constants $a = 4.16$ Å and $c = 6.76$ Å. On the assumption that the shapes of the growing nanocrystals correspond to the shape of the unit cell, we may consider cylindrical nanocrystals with diameter a and height c. The energy spectrum was calculated in [20] for cylindrical nanocrystals. The energy spectrum of the particle with a point defect on the end surface of the cylinder is similar to the spectrum of the defect-free sample. In this case, the edge of the absorption band is represented as

$$h\nu_{0.1} = E_{g0} + \frac{\hbar^2}{2\mu}\left(\frac{\lambda_{10}^2}{r^2} + \frac{\pi^2}{a^2}\right), \quad (4)$$

where $\lambda_{0.1} \approx 2.405$ and r and d are the radius and height of the cylinder, respectively.

The sizes of cylindrical nanocrystals are determined using expression (4) and ratio a/c. To compare the sizes with radius R of spherical nanocrystals, which enters expression (2), we consider a sphere with radius R^* the volume of which coincides with the volume of cylinder. The calculations show that ratio R/R^* is close to unity and virtually independent of the annealing time.

In the presence of the point defect, expression (4) is represented as

$$h\nu_{0.1} = E_{g0} + \frac{\hbar^2}{2\mu}\left(\frac{\lambda_{10}^2}{r^2} + \frac{y^2}{d^2}\right), \quad (5)$$

where quantity y depends on both amplitude and position of the δ-shaped potential. The calculations show that maximum y is reached at the given amplitude when the defect is located at the center of the cylinder. The above theoretical procedure was employed for the calculation of the shift of the absorption edge in the absence of the defect and in the presence of the defect at the center of the cylindrical nanocrystal. The shift can be up to 0.85 eV for the CdS_xSe_{1-x} samples ($r =$ 17.1 Å and $d = 27.8$ Å) the volume of which is equal to the volume of a sphere with radius $R = 18.3$ Å.

To interpret the observed features of the transmission spectra, we assume the presence of structural defects at the initial stage of the nanocrystal growth. Such defects provide a random potential that is added to the periodic potential of the crystal lattice. The further heat treatment leads to an increase in the degree of perfection of the crystal lattice.

The theoretical calculations of [20] show that the elimination of defects in the absence of variations in the sizes of nanocrystals may lead to the shift of the absorption edge by 0.85 eV. In the experiments, the 50-min heat treatment causes a shift of up to 0.3 eV. Such a shift cannot be interpreted using the diffusion growth of nanocrystals, since the diffusion coefficient in silicate glass is relatively low at a temperature of 530°C.

The spectral dependences of temperature coefficients of absorption dK/dT were studied in [22] for samples with different processing times at a temperature of 560°C. The theoretical spectral dependence of the absorption coefficient was obtained in [23] for the dielectric matrix containing semiconductor nanocrystals with the Gaussian size distribution. Such a dependence was used to calculate the spectral dependence of the temperature coefficient of absorption. The comparison of the theoretical and experimental curves yields the dependence of the variance of nanocrystals on the heat-treatment time (Fig. 8). The dependence of the variance of nanocrystals on the heat-treatment time also proves an increase in the degree of perfection of the crystal lattice in the course of thermal processing. Figure 8 shows that the heat treatment at a temperature of 560°C leads to a decrease in the variance at the initial stage and the further saturation. A similar dependence is obtained for a temperature of 420°C in spite of an insignificant variation in the size of nanocrystals at such a temperature. A decrease in the variance at relatively low heat-treatment temperatures can also be due to an increase in the perfection of the crystal lattice. At the initial stage of the growth of nanocrystals when the energy levels are broadened, the absorption edge cannot be sharp and the absorption in such systems is equivalent to the absorption in systems

with a relatively high variance of the sizes of nanocrystals.

CONCLUSIONS

We have fabricated CdS_xSe_{1-x} semiconductor nanocrystals in silicate glass and studied their optical transmission and photoluminescence spectra versus the degree of perfection of the crystal lattice. The shift of the absorption edge at the initial stage of the heat treatment is due to an increase in the degree of perfection of the crystal lattice in nanocrystals. Such a conclusion is proven by the theoretical calculations.

REFERENCES

1. Zh. Alferov, Rev. Mod. Phys. **73**, 767 (2001).
2. L. V. Asryan and R. S. Suris, Semiconductors **38**, 1 (2004).
3. X. Peng, L. Manna, W. Yang, J. Wickham, E. Scher, A. Kadavanich, and A. P. Alivisatos, Nature **404**, 59 (2000).
4. Y. Masumoto and T. Takagahara, *Semiconductor Quantum Dots* (Springer, Berlin, 2002).
5. N. Y. Morgan, C. A. Leatherdale, M. Drndic, Mirna V. Jarosz, Marc A. Kastner, and M. Bawendi, Phys. Rev. B **66**, 075339 (2002).
6. I. V. Bondar', V. S. Gurin, N. P. Solovei, and A. P. Molochko, Semiconductors **41**, 939 (2004).
7. A. I. Ekimov and A. L. Efros, Phys. Status Solidi B **150**, 627 (1988).
8. I. P. Suzdalev, *Nanotechnology: Physics and Chemistry of Nanoclasters, Nanostructures, and Nanomaterials* (Kom. Kniga, Moscow, 2006).
9. S. M. Brekhovskikh, Yu. P. Nikonov, and A. I. Neich, Fiz. Khim. Stekla **3**, 172 (1977).
10. L. E. Brus, Nanostruct. Mater. **1**, 71 (1992).
11. S. A. Gyrevich, A. L. Ekimov, I. A. Kudryavcev, O. G. Lublinskaya, and A. B. Osinski, Semiconductors **28**, 830 (1994).
12. L. Grigoryan, P. Petrosyan, S. Petrosyan, V. Bellani, and F. Maglia, Eur. Phys. J. B **34**, 415 (2003).
13. L. Grigoryan, P. Petrosyan, H. Petrosyan, and V. Bellani, Opt. Commun. **281**, 5838 (2008).
14. N. Kulish, V. Kunets, and M. Lisitsa, Ukr. Fiz. Zh. **37** (8), 114 (1992).
15. Y. Kayanuma, Phys. Rev. **38**, 9797 (1988).
16. I. Lifshits and V. Slezov, Zh. Eksp. Teor. Fiz. **35**, 479 (1958).
17. R. Kampman and R. Wagner, *Decomposition of Alloys: The Early Stages* (Pergamon, Oxford, 1983).
18. A. Forza and A. Selloni, *Tetrahedrally-Bonded Amorphous Semiconductors* (Plenum, New York–London, 1985), p. 271.
19. P. Nemec and P. Maly, J. Appl. Phys. **87**, 3342 (2000).
20. D. Sedrakyan, D. Badalyan, and L. Sedrakyan, Izv. Nats. Akad. Nauk Arm., Fiz. **49** (2), 71 (2014).
21. L. Grigoryan, P. Petrosyan, S. Petrosyan, V. Bellani, and F. Maglia, Eur. Phys. J. B **34**, 415 (2003).
22. Wei-Yu Wu, J. N. Schuiman, T. Y. Hsu, and Uzi Efron, Appl. Phys. Lett. **51**, 710 (1987).
23. D. Sedrakyan, P. Petrosyan, L. Grigoryan, and V. Badalyan, Tech. Phys. **56**, 1640 (2011).

Translated by A. Chikishev